RESEARCH ARTICLE SUMMARY

BLOOD-BRAIN BARRIER

Engineered Wnt ligands enable blood-brain barrier repair in neurological disorders

Maud Martin, Simon Vermeiren, Naguissa Bostaille, Marie Eubelen, Daniel Spitzer, Marjorie Vermeersch, Caterina P. Profaci, Elisa Pozuelo, Xavier Toussay, Joanna Raman-Nair, Patricia Tebabi, Michelle America, Aurélie De Groote, Leslie E. Sanderson, Pauline Cabochette, Raoul F. V. Germano, David Torres, Sébastien Boutry, Alban de Kerchove d'Exaerde, Eric J. Bellefroid, Timothy N. Phoenix, Kavi Devraj, Baptiste Lacoste, Richard Daneman, Stefan Liebner, Benoit Vanhollebeke*

INTRODUCTION: Central nervous system (CNS) endothelial cells establish a selective filter at the interface between the blood and the brain tissue, called the blood-brain barrier (BBB). The BBB is established during early embryogenesis and maintained throughout adulthood by neurovascular communications occurring within functionally integrated neurovascular units. In numerous CNS disorders, these homeostatic neurovascular microenvironments are disrupted, and consequently, excessive infiltrations of fluids, molecules, and cells alter the neuronal milieu and worsen disease outcome. Therapeutic strategies are needed for the restoration of compromised BBB function.

RATIONALE: An appealing strategy from a therapeutic standpoint is to repair the dysfunctional BBB by using the molecules that endogenously control its formation during embryogenesis. By respecting the developmental molecular logic of the target tissue, such an approach is best positioned to achieve physiological refunctionalization. More so, by focusing on the upstream regulators of BBB development, the likelihood of correctly setting the stage for a productive repair process increases. Wnt7a/b are some of the earliest and best characterized BBB-inducing signals across vertebrates and therefore constitute a priori prime candidates as BBB-repairing agents. Nonetheless, safe therapeutic use of Wnt ligands such as Wnt7a is unlikely because of their pleiotropic Frizzled (Fz) signaling activities and the widespread expression of Fz receptors across cells and tissues. However, at the BBB, Wnt7a/b ligands signal through an atypical receptor complex containing the adhesion G protein–coupled receptor Gpr124 and the glycosylphosphatidylinositol-anchored glycoprotein Reck. We reasoned that this receptor complex, more than the Fz receptors themselves, could be exploited to achieve BBB repair with the required level of specificity.

RESULTS: Wnt ligands exhibit a conserved two-domain structure, each domain making one functionally important contact with Fz receptors. We discovered that a hemisected Wnt7a, lacking the C-terminal domain and its embedded Fz contact site, retained partial but selective activity on the Gpr124/Reck-containing receptor complexes of the BBB. This specificity provided proof-of-concept evidence that the presence of Gpr124/Reck changes the modalities of Fz-Wnt interactions, and that Wnt7a/b can be used as scaffolds to achieve Gpr124/Reck-specific agonism. Accordingly, a class of highly specific and fully active Gpr124/Reck agonists, differing from Wnt7a by only a single surface-exposed residue, was identified through large-scale mutagenesis. Mechanistically, the selectivity of the uncovered agonists resulted from their strict dependency on Reck and Gpr124 for Fz binding and activation. In contrast to the wild-type Wnt7a ligand or other canonical Wnt ligands, whose overexpression is incompatible with vertebrate development, Gpr124/Reck agonists were well tolerated in vivo, even when delivered ubiquitously during *Xenopus* or zebrafish early development, or throughout the neonatal mouse brain. Furthermore, Gpr124/Reck agonists exhibited therapeutic efficacy in mouse models of brain tumors and ischemic stroke, where long-lasting BBB normalization was achieved through a single "hit-and-run" intravenous gene delivery. By restoring endothelial Wnt signaling, Gpr124/Reck agonists normalized the BBB pleiotropically, affecting both the transcellular and paracellular permeability pathways.

CONCLUSION: This work reveals that the signaling specificity of Wnt ligands is adjustable and defines a modality to treat CNS neurological disorders by normalizing BBB function. Such BBB-focused intervention strategies have considerable potential as disease-modifying treatments or as secondary preventive agents in various CNS pathologies, including stroke, multiple sclerosis, epilepsy, and neurodegenerative disorders such as Alzheimer's disease. ■

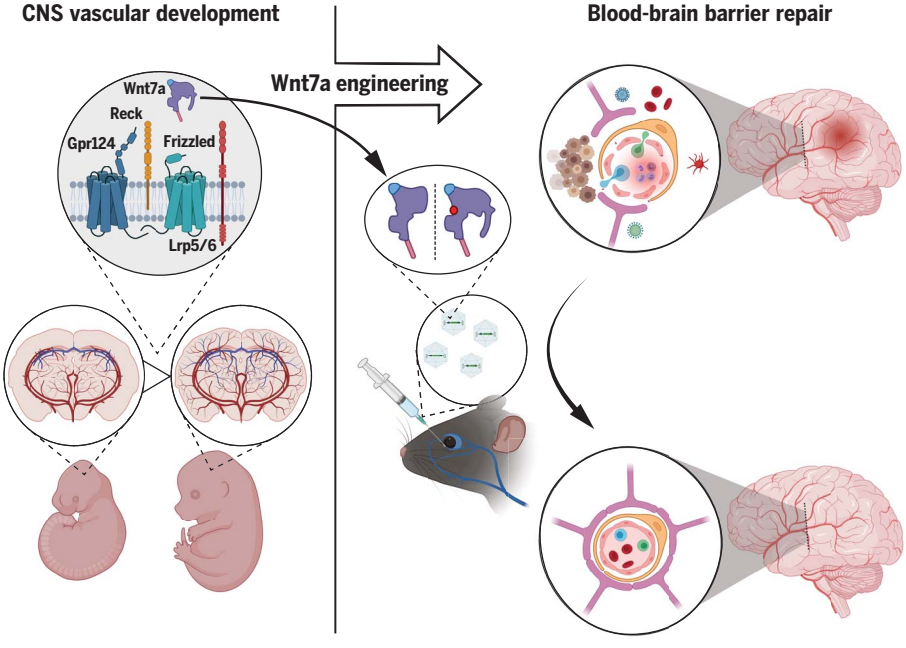

Repurposing Wnt7a ligands into BBB therapeutics. BBB dysfunction has been implicated in the etiology of a large set of CNS disorders. Wnt7a/b ligands, which dominate the neurovascular differentiation cascade during vertebrate development, are here repurposed as safe BBB therapeutics by engineering them into highly specific Gpr124/Reck agonists. [Illustration created with BioRender]

The list of author affiliations is available in the full article online.
*Corresponding author. Email: benoit.vanhollebeke@ulb.be
Cite this article as M. Martin *et al.*, *Science* **375**, eabm4459 (2022). DOI: 10.1126/science.abm4459

READ THE FULL ARTICLE AT
https://doi.org/10.1126/science.abm4459

RESEARCH ARTICLE

BLOOD-BRAIN BARRIER

Engineered Wnt ligands enable blood-brain barrier repair in neurological disorders

Maud Martin[1], Simon Vermeiren[1], Naguissa Bostaille[1], Marie Eubelen[1], Daniel Spitzer[2], Marjorie Vermeersch[3], Caterina P. Profaci[4], Elisa Pozuelo[5], Xavier Toussay[6], Joanna Raman-Nair[6], Patricia Tebabi[1], Michelle America[1], Aurélie De Groote[5], Leslie E. Sanderson[1], Pauline Cabochette[1], Raoul F. V. Germano[1], David Torres[7], Sébastien Boutry[3], Alban de Kerchove d'Exaerde[5], Eric J. Bellefroid[8], Timothy N. Phoenix[9], Kavi Devraj[2], Baptiste Lacoste[6], Richard Daneman[4], Stefan Liebner[2], Benoit Vanhollebeke[1,10]*

The blood-brain barrier (BBB) protects the central nervous system (CNS) from harmful blood-borne factors. Although BBB dysfunction is a hallmark of several neurological disorders, therapies to restore BBB function are lacking. An attractive strategy is to repurpose developmental BBB regulators, such as Wnt7a, into BBB-protective agents. However, safe therapeutic use of Wnt ligands is complicated by their pleiotropic Frizzled signaling activities. Taking advantage of the Wnt7a/b-specific Gpr124/Reck co-receptor complex, we genetically engineered Wnt7a ligands into BBB-specific Wnt activators. In a "hit-and-run" adeno-associated virus–assisted CNS gene delivery setting, these new Gpr124/Reck-specific agonists protected BBB function, thereby mitigating glioblastoma expansion and ischemic stroke infarction. This work reveals that the signaling specificity of Wnt ligands is adjustable and defines a modality to treat CNS disorders by normalizing the BBB.

Proper function of the central nervous system (CNS) requires a tightly controlled environment that safeguards the nervous system from harmful blood-borne components and pathogens. A blood-brain barrier (BBB) enables this separation via a selectively semipermeable boundary established by CNS vascular endothelial cells (ECs) that is induced and maintained by signals derived from other cells of the neurovascular unit, most notably pericytes and astrocytes (*1*–*5*).

BBB dysfunction displays varying degrees of cerebrovascular hyperpermeability, neurovascular uncoupling, or blood flow dysregulation; it has been linked to stroke, gliomas, epilepsy, traumatic brain injury, and neurodegenerative disorders (*1*, *3*, *5*, *6*). Upon BBB breakdown, leakage of neurotoxic plasma components, infiltration of immune cells, and CNS milieu alterations contribute to neuronal demise and worsen disease outcome (*4*, *5*). Because of their therapeutic potential across a wide range of disorders, clinically approved BBB-protective strategies are needed.

Among the many pathways that control neurovascular function, endothelial Wnt/β-catenin signaling acts as a master regulator of BBB physiology. It initiates the BBB differentiation cascade at the earliest steps of CNS vascular invasion and maintains BBB function in health and disease (*7*–*14*). Hence, identifying safe modalities to enhance Wnt/β-catenin signaling, selectively at the BBB, constitutes a promising therapeutic avenue for a range of neurological disorders.

Wnt/β-catenin–dependent BBB maturation is controlled by Wnt7a/b ligands (*7*–*9*), which therefore represent potential therapeutic agents to repair the dysfunctional BBB. However, the 19 Wnt ligands, including Wnt7a/b, interact promiscuously with the 10 Frizzled (Fz) receptors, with many Wnts able to engage a single Fz receptor and vice versa (*15*). Delivering Wnt7a/b ligands in vivo is thus predicted to have multiple adverse outcomes, including altered organogenesis, stem cell expansion, and tumorigenesis (*16*). Accordingly, Wnt7a overexpression is incompatible with proper vertebrate development. When expressed in *Xenopus* or zebrafish embryos, Wnt7a causes axis duplication or posteriorization of the anterior nervous system, respectively, which are classical dysmorphic outcomes of exacerbated Wnt/β-catenin signaling (fig. S1). This promiscuous signaling mode, together with the widespread Fz expression patterns and the difficulty in producing active Wnt proteins at bulk levels, has contributed to hampering the clinical development of Wnt signaling–based therapies.

In cerebral ECs, an atypical Wnt7a/b-specific co-receptor complex activates Wnt/β-catenin signaling during brain angiogenesis and BBB regulation (*17*, *18*). This co-receptor complex contains the glycosylphosphatidylinositol-anchored glycoprotein Reck and the adhesion G protein–coupled receptor Gpr124. Wnt7a/b thus activates two distinct types of membrane receptor complexes. One has broad tissue distribution and binds nondiscriminately to Wnt7a/b and other Wnt ligands via two contact sites with Fz and a third interaction with Lrp5/6 (Fig. 1A, hereafter termed the systemic "off-target" complex). The other complex is enriched at the level of the BBB ECs and is highly specific for Wnt7a/b. In this case, Reck provides an additional contact point by binding at least in part to the divergent linker peptide of Wnt7a/b (Fig. 1A, BBB "on-target"). After physically binding to Wnt7a/b, Reck stabilizes the ligand in a signaling-competent lipophilic conformation and delivers it to Fz receptors via the transmembrane tethering function of Gpr124. Thereby, Reck and Gpr124 synergistically stimulate Wnt7a/b-specific responses by assembling higher-order Gpr124/Reck/Fz/Lrp5/6 complexes (*19*–*21*).

Discovery of highly specific Gpr124/Reck agonists

Taking advantage of the differential composition of these receptor complexes, we attempted to selectively target the BBB by engineering Wnt7a/b into Gpr124/Reck-specific agonists. To that end, we determined which Fz receptors are competent for Wnt7a/b signaling in Wnt/β-catenin–reporting super top flash (STF) HEK293(T) cells (fig. S2). Wnt7a and Wnt7b signaled preferentially through Fz5 and Fz8 in wild-type or *GPR124*$^{-/-}$;*RECK*$^{-/-}$ cells (fig. S2, A and B, and table S1). Upon Gpr124 and Reck overexpression in wild-type cells, Wnt7a/b signals were selectively and potently stimulated even in the absence of a coexpressed Fz, probably because of confounding endogenous expression of Fz (fig. S2C and table S1). In a *GPR124*$^{-/-}$;*RECK*$^{-/-}$;*FZ*$_{1\text{-}10}^{-/-}$ CRISPR/Cas9 null genetic background, Fz5 and Fz8 were confirmed as the only Wnt7a/b receptors signaling in the absence of Gpr124/Reck, whereas most Fz receptors proved competent for Gpr124/Reck-dependent signaling (fig. S3). If we assume similar expression and localization of the ectopically expressed Fz receptors, Wnt7a/b thus signal through distinct Fz receptors depending on the absence or presence of Gpr124/Reck (Fig. 1A).

[1]Laboratory of Neurovascular Signaling, Department of Molecular Biology, ULB Neuroscience Institute, Université libre de Bruxelles, Gosselies B-6041, Belgium. [2]Institute of Neurology (Edinger Institute), University Hospital, Goethe University Frankfurt, Frankfurt am Main, Germany. [3]Center for Microscopy and Molecular Imaging, Université libre de Bruxelles, Université de Mons, Gosselies B-6041, Belgium. [4]Departments of Pharmacology and Neurosciences, University of California, San Diego, La Jolla, CA, USA. [5]Laboratory of Neurophysiology, ULB Neuroscience Institute, Université libre de Bruxelles, Brussels B-1070, Belgium. [6]Ottawa Hospital Research Institute, Neuroscience Program, Department of Cellular and Molecular Medicine, University of Ottawa Brain and Mind Research Institute, Faculty of Medicine, Ottawa, Ontario, Canada. [7]Institut d'Immunologie Médicale, Université libre de Bruxelles, Gosselies, Belgium. [8]Laboratory of Developmental Genetics, ULB Neuroscience Institute, Université libre de Bruxelles, Gosselies B-6041, Belgium. [9]Division of Pharmaceutical Sciences, James L. Winkle College of Pharmacy, University of Cincinnati, Cincinnati, OH, USA. [10]Walloon Excellence in Life Sciences and Biotechnology (WELBIO), Wavre, Belgium.
*Corresponding author. Email: benoit.vanhollebeke@ulb.be

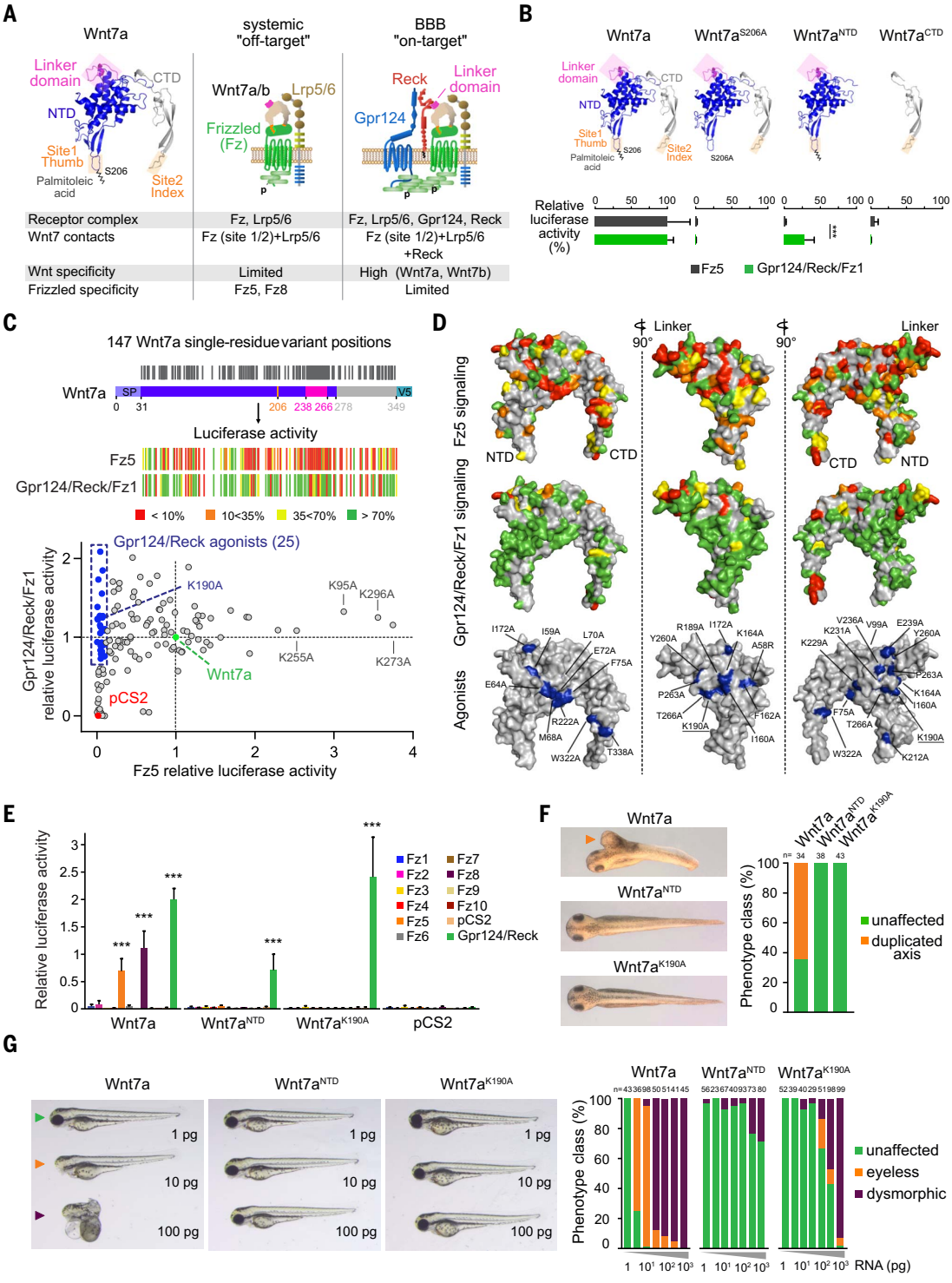

Fig. 1. Engineering Wnt7a ligands into highly specific Gpr124/Reck activators. (**A**) Backbone model of murine Wnt7a based on the crystal structure of XWnt8a (*15*) and schematics of the receptor complexes mediating Wnt7a/b/β-catenin signaling. (**B**) Relative STF (super top flash) luciferase activity of Wnt7a and its depicted variants on Fz5 or Gpr124/Reck/Fz1. (**C**) Position and color-coded Gpr124/Reck/Fz1 or Fz5 STF activities of 147 V5-tagged single-residue Wnt7a variants. Gpr124/Reck agonists (blue dots) were defined as variants with >70% Gpr124/Reck/Fz1 and <10% Fz5 activity. (**D**) Front, lateral, and back views of the Wnt7a surface model with integrated color-coded activities of all 147 single-residue variants. Agonists are in blue. (**E**) β-Catenin signaling assays using STF cells transfected with any of the 10 Fz receptors or Gpr124/Reck, together with Wnt7a, Wnt7a^{NTD}, Wnt7a^{K190A}, or the empty pCS2 vector. (**F**) Phenotypic scoring of stage 36 *Xenopus laevis* embryos injected into the ventral vegetal region of the four-cell embryo with 15 pg of the indicated mRNA. Arrowhead indicates duplicated axis. (**G**) Phenotypic scoring of 3-dpf zebrafish larvae injected at the one-cell stage with Wnt7a, Wnt7a^{NTD}, or Wnt7a^{K190A} mRNA at the indicated doses. Colored arrowheads refer to the phenotypic classes on the right. Wnt7a and variants are V5-tagged. Data are means ± SD. ***P < 0.001. Amino acid abbreviations: A, Ala; E, Glu; F, Phe; I, Ile; K, Lys; L, Leu; M, Met; P, Pro; R, Arg; T, Thr; V, Val; W, Trp; Y, Tyr.

The near-uniform competence of Fz isoforms for Gpr124/Reck-dependent Wnt7a/b signaling reveals that these ligands lose their capacity to distinguish Fz receptors when bound by Reck within the Gpr124/Reck/Fz/Lrp5/6 complex. Because Wnt ligands discriminate Fz receptors primarily via site 2 (*15*), we suspected that Wnt7a/b activity at the BBB might be dominated by site 1 of the N-terminal domain (NTD). Supporting this hypothesis, chimeric Wnt ligands composed of Wnt7a NTD fused to a C-terminal domain (CTD) derived from another Wnt were competent for Reck binding and Gpr124/Reck-dependent signaling (fig. S4) (*19*, *21*).

This suggested that in contrast to the systemic "off-target" situation, where both contact sites 1 and 2 are strictly required for Wnt signaling, Wnt7a/b-Fz interaction at site 2 might become dispensable in the context of Gpr124/Reck-stimulated signaling. Accordingly, Wnt7a^{NTD}, a hemisected Wnt7a variant, retained partial activity on Gpr124/Reck/Fz1-mediated signaling while showing no stimulation of Fz5 signaling, used as a paradigm "off-target" readout (Fig. 1B). Furthermore, mutating three of the five Wnt7a residues involved

in site 2 contacts did not affect Gpr124/Reck-mediated signaling while reducing Fz5 signaling by more than 50% (fig. S5). Both Wnt7a^{CTD} and Wnt7a^{S206A}, with impaired site 1, were fully inactive. These findings show that altering the structure of Wnt ligands can modulate their signaling specificity, and more specifically, that Wnt7a can be engineered into a Gpr124/Reck-specific ligand.

On the basis of this proof of concept, we implemented a large-scale screen for Gpr124/Reck-specific Wnt7a variants with optimal "on-target" activity because Wnt7a^{NTD} is only ~30% as active as the parental Wnt7a ligand. We generated a collection of 147 single-residue variants of V5-tagged murine Wnt7a, mostly through alanine substitutions. This collection corresponds to 46% of the residues of the secreted protein and 51% of its exposed surface. Each variant was tested for its Gpr124/Reck-dependent and -independent activity (Fig. 1, C and D, fig. S6A, and table S2). Wnt7a/Fz5 signaling appeared highly sensitive to Wnt7a mutations, with 37% of the variants exhibiting <10% activity and only 31% maintaining >70% activity. Most tested inactive variants (15/17) showed levels of extracellular accumulation similar to those of Wnt7a, ruling out improper trafficking as a leading cause for the large proportion of Fz5-inactive variants (fig. S7). In contrast to Fz5, Gpr124/Reck signaling appeared homogeneous and largely insensitive to Wnt7a variations, as 76% of the variants retained >70% activity (Fig. 1, C and D, and fig. S6A).

This led to the identification of 25 single-residue variants displaying highly specific Gpr124/Reck activity (so-called "agonists" >70% on-target, <10% off-target; Fig. 1, C and D, fig. S6B, and table S2). Wnt7a^{K190A} was selected as a single-residue Gpr124/Reck agonist prototype, optimally combining a wild type–like signal on Gpr124/Reck and undetectable "off-target" Fz5 activity.

In vitro, none of the transfected Fz receptors could be stimulated by Wnt7a^{NTD} or Wnt7a^{K190A} in the absence of Gpr124/Reck (Fig. 1E). In vivo, contrary to Wnt7a, ubiquitous expression of Wnt7a^{NTD} or Wnt7a^{K190A} after mRNA injections failed to trigger gross morphological alterations in *Xenopus* or zebrafish (Fig. 1, F and G). Although the in vivo expression level and secretion rate were not formally compared, dose response experiments in zebrafish revealed that 3 pg of Wnt7a mRNA was sufficient to trigger "off-target" signaling, whereas Wnt7a^{NTD} and Wnt7a^{K190A} were well tolerated even when expressed in a 100-fold excess (Fig. 1G). Wnt7a signaling in this setting is Gpr124-independent, as revealed by the analysis of zygotic and maternal-zygotic *gpr124^{s984}* mutants (*17*) (fig. S1C). As a control, in Gpr124/Reck-overexpressing zebrafish embryos, Wnt7a or Wnt7a^{K190A} triggered morphological alterations at low mRNA doses (fig. S8).

Gpr124/Reck agonists require Reck to bind Fz

Mechanistically, the selectivity of the uncovered agonists resulted from their incapacity to bind, and therefore activate, Fz receptors in the absence of Gpr124/Reck. Indeed, whereas Wnt7a immunolocalized to the surface of *RECK$^{-/-}$;GPR124$^{-/-}$* cells transiently transfected with Reck or Fz5, Wnt7a^{NTD} and Wnt7a^{K190A} labeled the membrane in the presence of Reck, but not Fz5 (Fig. 2, A and B). Accordingly, the agonists coimmunoprecipitated with hemagglutinin (HA)–tagged Reck as efficiently as did Wnt7a (Fig. 2C) but failed to bind HA-Fz5 in *RECK$^{-/-}$* cells unless Reck was coexpressed (Fig. 2D).

The distant position of the agonistic K190A mutation on the Wnt7a structure makes it unlikely that K190A directly affects the interaction with Fz. Instead, such a mutation could affect the biophysical properties of the ligand. Wnt ligands are indeed short-lived and rapidly lose activity by oligomerization, in a process that increases their hydrosolubility (*22*, *23*). Reck has been shown to extend the half-life of Wnt7a activity by maintaining it in a monomeric, hydrophobic state (*20*, *24*). It is thus possible that the introduction of single-residue variations into Wnt7a reduces ligand stability below a threshold required for Fz signaling, a property that the stabilizing action of Reck could counteract. In agreement with this idea, a clear correlation was seen at the single-residue level between Fz5 and Gpr124/Reck/Fz1 activities when assessed across the 147 Wnt7a variants. Variants displaying even slightly reduced activity on Gpr124/Reck (yellow, orange, or red residues in Fig. 1, C and D) were generally fully inactive in the more sensitive Fz5 setting (Fig. 2E). Conversely, preservation of at least partial Fz5 activity (orange, yellow, or green residues in Fig. 1, C and D) strongly correlated with full activity on Gpr124/Reck (Fig. 2E).

The stability of morphogens influences their range of action, with more stable ligands capable of activating more distant cells. We analyzed the capacity of Wnt7a and Wnt7a^{K190A} to activate Wnt signaling at short distances (autocrine monocultures) versus longer distances (paracrine cocultures) (Fig. 2F). Although Wnt7a exhibited partial paracrine activity, Wnt7a^{K190A} could not reach the receiving cell in an active form. The whole collection of agonists behaved similarly in this assay (fig. S9). Furthermore, combining agonistic mutations almost invariably resulted in fully inactive ligands, even when tested on Gpr124/Reck signaling in monocultures (Fig. 2G). Conversely, introducing K95A, K255A, K273A, and K296A mutations into Wnt7a^{K190A} (all of which increase Fz5 activity; Fig. 1C) was sufficient to abolish selectivity by restoring partial Fz5 signaling (Fig. 2H). Finally, mutating Lys^{190} to alternative residues (Gly, Ser, Leu, Pro, Asp, Glu, or Arg) had variable effects on signaling specificity (Fig. 2I). In sum, by recruiting Wnt7a/b into a higher-order receptor complex, Gpr124/Reck profoundly redefines the Wnt7a/b primary structure requirements for Fz signaling.

Activity of Gpr124/Reck agonists in zebrafish

To test the functionality of the agonists in vivo, we first generated a genetic deficiency model in zebrafish. Morpholino-mediated gene knockdown and in situ hybridization of the four zebrafish Wnt7a/b paralogs identified *wnt7aa* as the BBB-relevant ligand (fig. S10). We therefore generated *wnt7aa^{ulb2}*, a CRISPR/Cas9 frame-shift allele (Fig. 3A). *gpr124* mutants (*17*) and homozygous *wnt7aa^{ulb2}* mutants (*wnt7aa$^{-/-}$*) display similar cerebrovascular and dorsal root ganglia (DRG) neurogenesis defects (Fig. 3B) and lack Wnt/β-catenin reporter expression in CNS-invading vessels (Fig. 3C). In cell cultures, all tested human, mouse, and zebrafish orthologs of the Wnt7/Gpr124/Reck signaling module were functionally interchangeable (fig. S11), supporting the functional assessment of murine ligands in zebrafish.

The *wnt7aa$^{-/-}$* DRG defects could be partially corrected by injecting 100 pg of Wnt7a^{NTD} or Wnt7a^{K190A} mRNA at the one-cell stage. By contrast, Wnt7a was toxic at equivalent doses (Figs. 1G and 3D). *Wnt7aa$^{-/-}$* cerebrovascular phenotypes could not be rescued by mRNA injections, presumably as a result of the late onset of zebrafish hindbrain angiogenesis (36 hpf). Therefore, we adopted a mosaic transgenic endothelial expression strategy using a *kdrl* (*vegfr2*) promoter. In this approach, Wnt7a^{K190A} restored the formation of central arteries (CtAs) to a level comparable to Wnt7a, and these vessels expressed glucose transporter–1 (Glut1), a marker of BBB maturation (Fig. 3E). Reflecting its partial activity in vitro, Wnt7a^{NTD} was less potent.

These results, demonstrating the capacity of the agonists (in particular Wnt7a^{K190A}) to stimulate Wnt signaling at the BBB, led us to test their protective potential in a zebrafish atorvastatin (ATV)–induced hemorrhagic stroke model, reminiscent of human cerebral cavernous malformation (CCM)–like lesions (*25*). Although more than 90% of ATV-exposed wild-type larvae displayed moderate to severe intracranial (IC) hemorrhages, transgenic endothelial expression of Wnt7a^{K190A} decreased the extent of cerebrovascular ruptures, with more than half of the embryos showing no or little bleeding (Fig. 3F). ATV also caused the accumulation of intracardially injected 10-kDa dextran into the hindbrain (Fig. 3G). Wnt7a^{K190A} expression could as well counteract these more subtle ATV-induced BBB defects, as revealed by the examination of embryos expressing Wnt7a^{K190A} hemispherically (Fig. 3H).

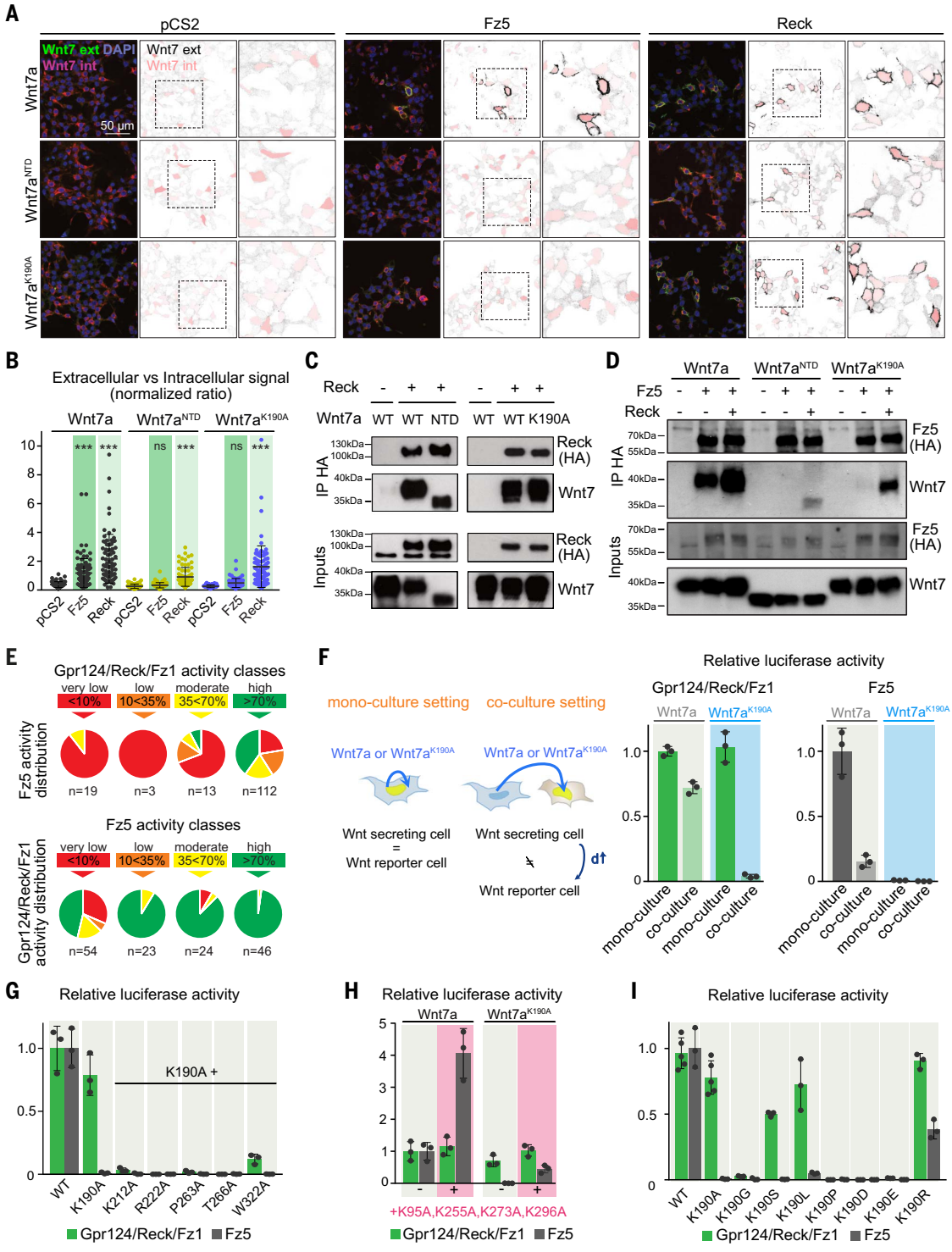

Fig. 2. Gpr124/Reck agonists are unable to bind Fz autonomously. (**A**) *GPR124*$^{-/-}$;*RECK*$^{-/-}$ HEK293 cells transiently expressing Wnt7a, Wnt7a^{NTD}, or Wnt7a^{K190A} together with Fz5, Reck, or the empty pCS2 vector were submitted to Wnt7a double immunostaining, before (Wnt7a extracellular, green/black) and after (Wnt7a intracellular, pink) cell permeabilization. (**B**) Quantification of (A), as described in the supplementary materials. (**C** and **D**) Anti-HA coimmunoprecipitation assays after membrane-impermeable cross-linking in total lysates of *RECK*$^{-/-}$ HEK293T cells expressing HA-Reck (C) or HA-Fz5 (D) together with Wnt7a, Wnt7a^{NTD}, or Wnt7a^{K190A}, with or without expression of untagged Reck (D). (**E**) Gpr124/Reck/Fz1 and Fz5 activity correlations across the Wnt7a single-residue variants collection. (**F**) Relative STF luciferase activity in the presence of Gpr124/Reck/Fz1 or Fz5 in response to Wnt7a or Wnt7a^{K190A} in autocrine monoculture or paracrine coculture variants settings. (**G** to **I**) Gpr124/Reck/Fz1 or Fz5 STF activities of Wnt7a^{K190A} with combined agonistic mutations (G), activity-increasing mutations (H), or alternative substitutions of Lys^{190} (I). Wnt7a and variants are V5-tagged. Data are means ± SD. ***P < 0.001; ns, nonsignificant.

Brainwide delivery of Gpr124/Reck agonists in mice

We next evaluated Gpr124/Reck agonists as BBB-protective agents in mammals. To deliver the agonists widely throughout the mouse CNS, we generated PHP.eB adeno-associated viruses expressing enhanced green fluorescent protein (AAV-EGFP), Wnt7a-P2A-EGFP (AAV-Wnt7a), or Wnt7a^{K190A}-P2A-EGFP (AAV-K190A) under the control of a constitutive CAG promoter. Upon intravenous injection of 4×10^{11} vg (viral genomes) in 8-week-old mice, CD31-positive brain vessels were surrounded by EGFP^{+} cells (Fig. 4A), exposing ECs to local sources of Wnt7a or Wnt7a^{K190A}. The AAV-PHP.eB capsid drives expression of the transgenes in ~25% of ECs, ~30% of astrocytes, and ~45% of NeuN^{+} neurons (fig. S12A), as reported previously (*26*). More than 95% of the desmin^{+} pericytes were negative for EGFP. Pericytes are thus, at best, marginal sources of Wnt7a in this approach (fig. S12B).

Although expressed from widely distributed cells, Wnt7a and Wnt7a^{K190A} showed a more discrete distribution, with preferential accumulation at the level of CD31-positive vessels, as well as some scattered parenchymal cells

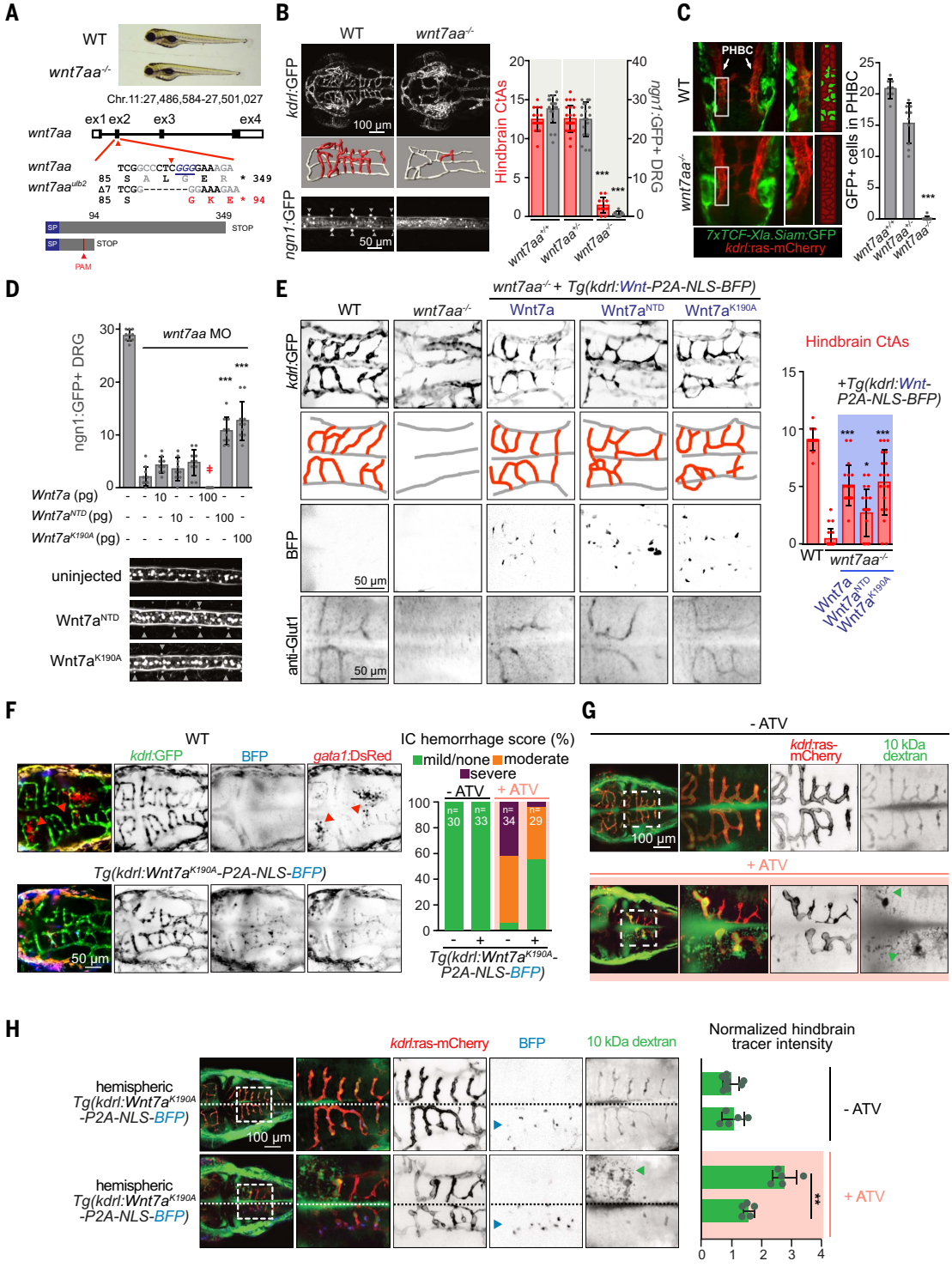

Fig. 3. Gpr124/Reck agonists stimulate brain angiogenesis, promote blood-brain barrier induction, and prevent hemorrhagic stroke in zebrafish. (**A**) Characterization of the *wnt7aa*^{ulb2} allele. PAM, protospacer adjacent motif. (**B**) 60-hpf *Tg(kdrl:GFP)* hindbrain CtAs (central arteries) and 72-hpf *Tg(neurog1:GFP)* dorsal root ganglia (DRG, gray arrowheads) in wild-type (WT) and *wnt7aa* mutant zebrafish. (**C**) 30-hpf WT and *wnt7aa* mutant *Tg(7xTCF-Xia.Siam:GFP);Tg(kdrl:ras-mCherry)* hindbrains and quantification of GFP^{+} (β-catenin signaling–positive) ECs in the perineural PHBCs (primordial hindbrain channels). (**D**) DRG in 72-hpf *wnt7aa* morphants injected at the one-cell stage with the indicated mRNAs. Injection of 100 pg of Wnt7a mRNA is developmentally toxic (‡). (**E**) 48-hpf WT and *wnt7aa*$^{-/-}$ *Tg(kdrl:GFP)* hindbrain cerebrovasculatures, with transgenic endothelial expression of Wnt7a, Wnt7a^{NTD}, or Wnt7a^{K190A}. BFP is used as a transgenesis marker; Glut1 immunostaining illustrates BBB differentiation. (**F**) Intracerebral (IC) hemorrhage score of 54 hpf *Tg(kdrl:GFP);Tg(gata1a:dsRed)* embryos treated from 34 hpf onward with 1 μM atorvastatin (ATV), with or without transgenic endothelial expression of Wnt7a^{K190A}. Red arrowheads point to extravasated erythrocytes. (**G**) BBB leakage of 10-kDa dextran upon ATV exposure. (**H**) Quantification of 10-kDa dextran tracer leakage upon ATV exposure, with or without hemispheric transgenic endothelial expression of Wnt7a^{K190A} in 54-hpf embryos. Data are means ± SD. *P < 0.05, **P < 0.01, ***P < 0.001.

(Fig. 4B, asterisks). The distribution of the ligands, and hence their potential activity, likely reflects the expression patterns of their receptors, with unbound ligands getting cleared through the glymphatic system (*27*) or other routes. Accordingly, Wnt7a exhibited a more significant nonvascular distribution (Fig. 4B, asterisks). More so, immunodetection of β-catenin activity (LacZ signal) in coronal brain sections of BAT-GAL mice (*28*) revealed that, in contrast to Wnt7a^{K190A}, Wnt7a triggered ectopic Wnt/β-catenin signaling in non-endothelial cells of the hippocampus (dentate gyrus) and the parafascicular nucleus of the thalamus at all examined time points [7, 14, and 28 days post-injection (dpi)] (Fig. 4C). These two areas are associated with Fz5 expression (*29*, *30*). Other brain regions did not exhibit increased LacZ signal (fig. S13). The BAT-GAL results were confirmed using RNAScope hybridization of the Wnt target *Axin2* (Fig. 4D and fig. S14).

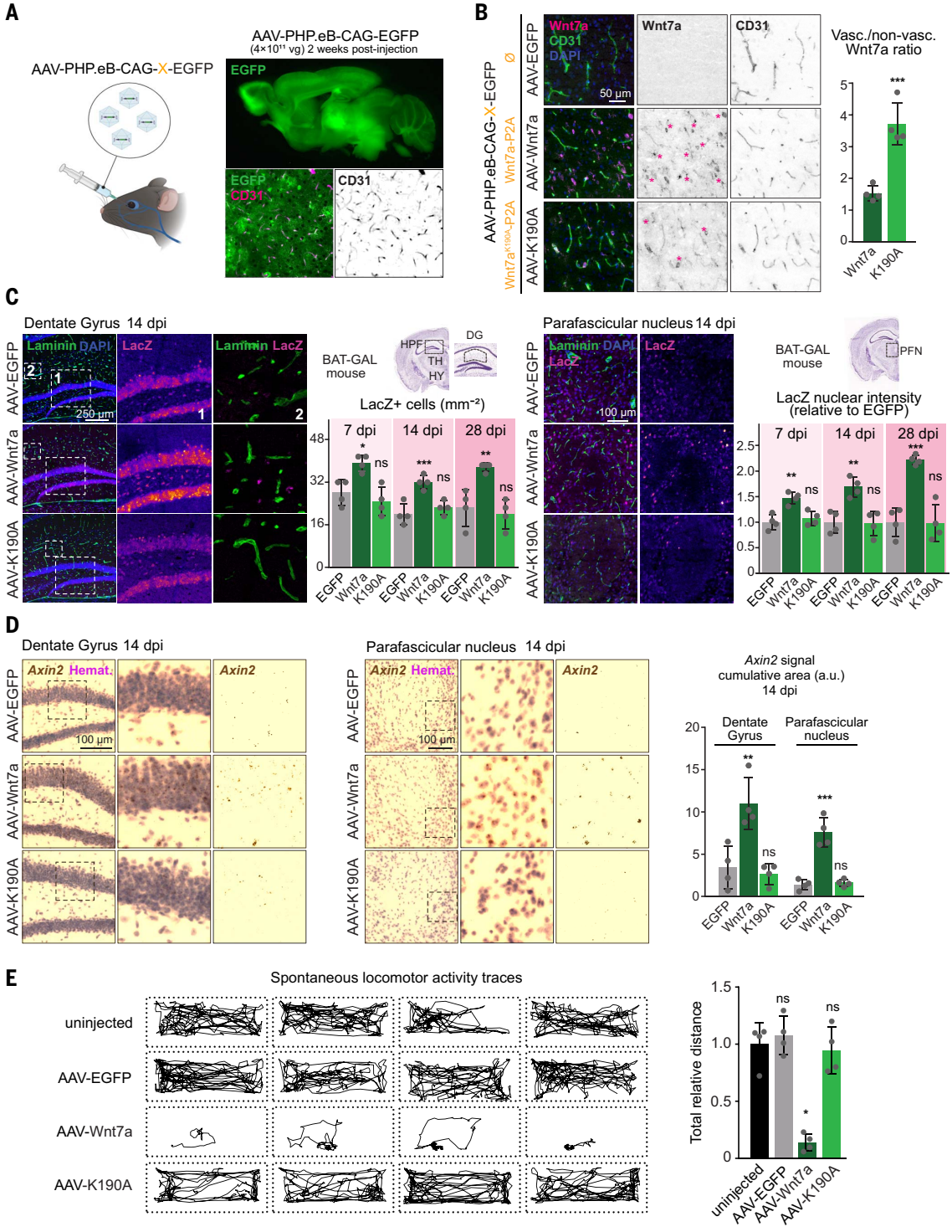

Fig. 4. Absence of ectopic Wnt activities or behavioral defects after brainwide AAV-mediated gene delivery of Gpr124/Reck agonists in mice. (**A** and **B**) Immunostaining of sagittal brain sections for EGFP and CD31 (vessels) (A) and coronal sections for Wnt7a or its variant and CD31 together with a DAPI counterstain (B), 2 weeks after intravenous injections of the indicated AAVs. (**C**) Staining of coronal sections of AAV-injected BAT-GAL mice for LacZ, laminin, and DAPI in the hippocampal area dorsal to the dentate gyrus (DG, left) and in the parafascicular nucleus area (PFN, right). Nuclear LacZ-positive cells or signal intensities were quantified at 7, 14, and 28 days post-injection (dpi). HPF, hippocampal formation; TH, thalamus; HY, hypothalamus. (**D**) RNAScope in situ hybridization of *Axin2* in coronal sections of AAV-injected WT mice. (**E**) Spontaneous open-field locomotor activity traces of postnatal day 20 (P20) mice injected retro-orbitally at P2 with 4×10^{10} vg of the indicated AAV-PHP.eB viruses. Spontaneous locomotor activity is quantified as the distance traveled for 3 min; data are means ± SD. $^{*}P < 0.05$, $^{**}P < 0.01$, $^{***}P < 0.001$.

Although the ectopic Wnt7a activities did not result in obvious behavioral defects in adult mice (fig. S15), gene delivery of Wnt7a, but not Wnt7a^{K190A} or EGFP, was detrimental to neonatal spontaneous locomotor activity (Fig. 4E). We next assessed the Wnt activity status at the target BBB endothelium by staining for lymphoid enhancer binding factor 1 (LEF1) because the low Wnt activity levels of adult BBB ECs are not detectable using BAT-GAL reporter mice (fig. S13) (*31*). AAV-based delivery of Wnt7a or Wnt7a^{K190A} did not increase LEF1 signals in healthy ECs (fig. S16).

A "hit-and-run" gene delivery of Gpr124/Reck agonists in glioblastoma multiforme

The absence of "off-target" Wnt signaling activity after widespread Wnt7a^{K190A} expression in the mouse brain prompted us to test its therapeutic potential in CNS pathologies associated with BBB dysfunction, starting with glioblastoma multiforme (GBM). GBM, the most aggressive and frequent primary brain tumor, is characterized by a dense vascular network exhibiting disrupted BBB properties, and endothelial Wnt signaling has been reported to control vascular integrity in this and other

brain tumors (*12*, *14*, *32*, *33*). Two days after orthotopic implantation of 1×10^5 GL261 tumor cells into the C57BL/6 mouse striatum, we performed a single "hit-and-run" intravenous AAV-PHP.eB gene delivery and monitored tumor volume by magnetic resonance imaging (MRI) at 21 to 24 days post-implantation (dpi) (Fig. 5A). Although control tumor expansion was highly variable, with volumes ranging from 10 to 80 mm^3, $Wnt7a^{K190A}$ expression (AAV-K190A) reduced this variability and limited tumor volume to ~20 mm^3. In particular, the proportion of larger tumors (>40 mm^3) was reduced (8% in K190A versus 33% in controls).

At 25 dpi, mice with the largest tumors started to exhibit disease symptoms, including faulty postural syndromes and abnormal gait. This time point was therefore chosen for terminal analysis and tissue harvesting. Control tumors exhibited more prominent microvascular hemorrhages (asterisks) and edema than did AAV-K190A tumors (Fig. 5B), suggesting cerebrovascular differences between the groups. Accordingly, the K190A tumor-associated vasculature showed features of vessel normalization, such as reduced $CD31^+$ vascular density (Fig. 5C), fewer large vessels (Fig. 5C), and

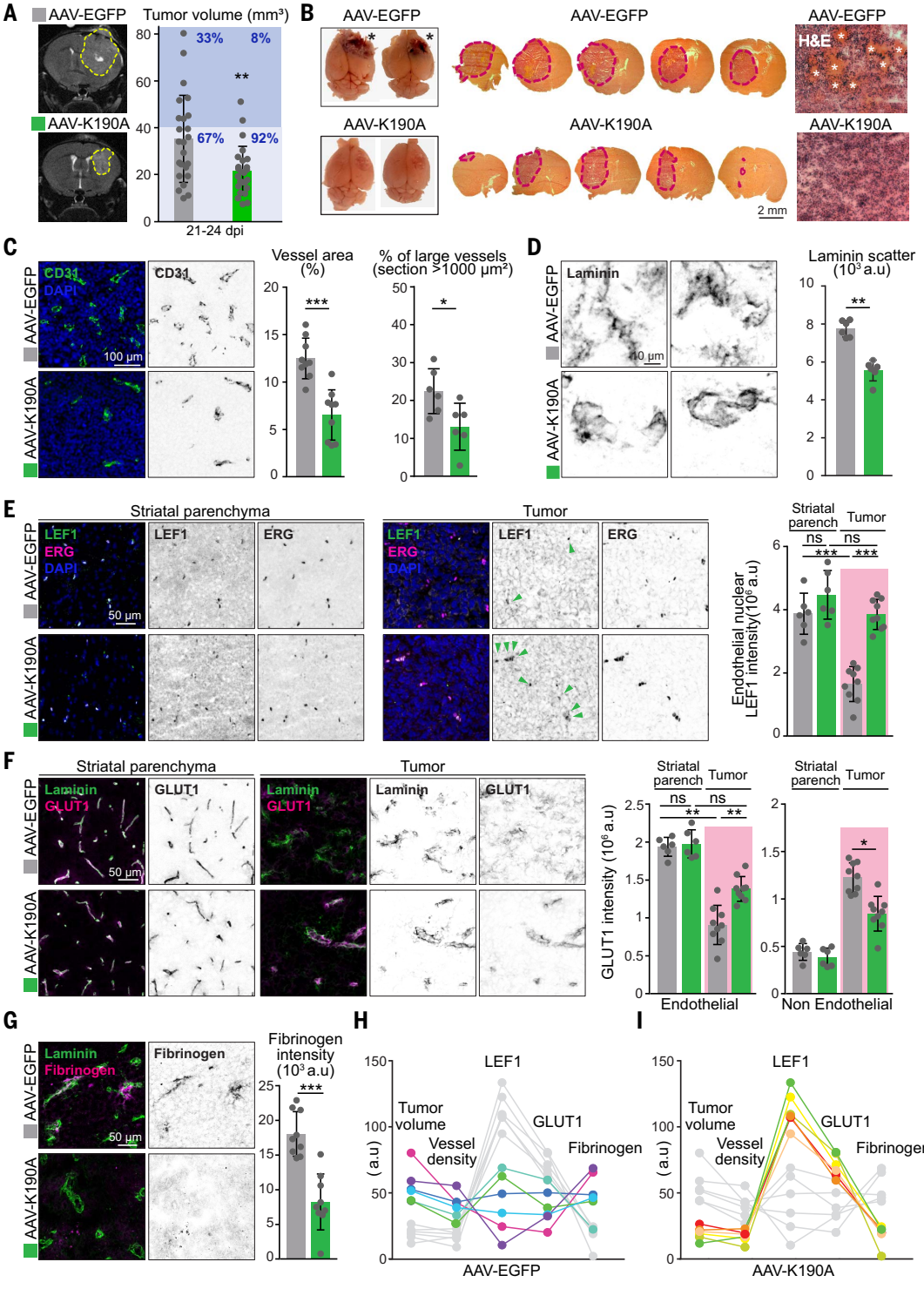

Fig. 5. A single "hit-and-run" gene delivery of Gpr124/Reck agonists achieves neurovascular-specific Wnt/β-catenin activation and vessel normalization in glioblastoma multiforme. (**A**) GL261-implanted mice, injected intravenously at 2 dpi (days post-implantation) with 4×10^{11} to 1×10^{12} vg of AAVs, were imaged by MRI to evaluate tumor volumes between 21 and 24 dpi. The dashed lines highlight the tumor margin. (**B**) At 25 dpi, mice were euthanized for brain gross morphology assessment (left) and H&E staining of serial sections (center and right). Asterisks indicate hemorrhages. (**C** to **G**) Coimmunostaining of tumor or parenchymal (parench) 25-dpi coronal sections for ECs (CD31) (C), vascular basement membranes (laminin) (D), LEF1 together with the endothelial nuclear marker ERG (E), GLUT1 together with laminin (F), or fibrinogen together with laminin (G). (**H**) Correlation between endothelial Wnt activity (LEF1) and tumor volume, vessel density, GLUT1, and fibrinogen leakage in tumors of AAV-EGFP–injected mice (colored lines). (**I**) Same as (H) in AAV-K190A–injected mice. Data are means ± SD; a.u, arbitrary units. *$P < 0.05$, **$P < 0.01$, ***$P < 0.001$.

more compact and smoother distribution of laminin (Fig. 5D). Cell densities were comparable in AAV-EGFP and AAV-K190A tumors (6425 versus 7141 cells mm^{-2}, respectively), implying that differential tumor volumes are more prominently explained by altered tumor cell proliferation than by vasogenic edema. Nuclear LEF1 staining revealed the low endothelial Wnt signaling activity typically associated with GBM vessels (Fig. 5E) (*14*). $Wnt7a^{K190A}$ restored Wnt activity in the tumor endothelium, to a level similar to the steady-state activity of nontumoral parenchymal vessels. In contrast, it did not significantly affect LEF1 levels in vessels of the contralateral hemisphere (Fig. 5E), confirming the findings in healthy mice (fig. S16). In agreement with nuclear LEF1 accumulation, BBB integrity was partially restored in tumor vessels, as revealed by increased GLUT1 immunoreactivity (Fig. 5F) and reduced fibrinogen extravasation (Fig. 5G). The restoration of GLUT1 signal in GBM vessels was accompanied by reduced tumor parenchymal GLUT1, paralleling the developmental switch of GLUT1 expression from the neuroepithelium to the vessels upon CNS vascularization (*8*, *9*).

To determine the source of $Wnt7a^{K190A}$ within the tumor microenvironment, we monitored the distribution of the coexpressed EGFP (fig. S17). Glioblastoma cells were negative, as expected from the nonreplicative nature of AAV genomes and the numerous cell divisions of these cells upon implantation. Within the tumor, 30% of $CD31^+$ endothelium was $EGFP^+$, and blood vessels accounted for ~60% of the total intratumoral $EGFP^+$ signal. In addition, the EGFP signals were particularly intense in $S100\beta^+/GFAP^-$ astrocytes of the tumor glial scar, whereas $Iba1^+$ microglia were $EGFP^-$.

These discrete $Wnt7a^{K190A}$ sources resulted in relatively uniform effects on tumor growth. By contrast, control GL261 tumors exhibited more significant heterogeneity (Fig. 5A). We reasoned that this heterogeneity could reflect differences in endothelial Wnt signaling levels. In agreement, endothelial LEF1 and GLUT1 levels in control tumors inversely correlated with vessel density, fibrinogen leakage, and tumor volume (Fig. 5H). These correlations suggest that the growth rate of GL261 tumors is at least partially determined by the level of residual Wnt signaling of its perfusing vasculature, and that AAV-delivery of $Wnt7a^{k190A}$ is sufficient to uniformly raise the signaling level to promote neurovascular normalization and tumor growth reduction (Fig. 5I).

Gpr124/Reck agonists as BBB repair agents in glioblastoma and stroke models

The variable degree of residual endothelial Wnt signaling within the wild-type GL261 tumor endothelium complicated the analysis of the mechanism underlying endothelial Wnt-induced BBB repair. Therefore, we resorted to transgenic Tet-Off GL261 cells that conditionally express the secreted Wnt inhibitor Dkk1 (dickkopf WNT signaling pathway inhibitor 1) (*12*). When exposed to doxycycline, these cells potently repress Dkk1 expression in vitro and in vivo without affecting their intrinsic in vitro growth rate (fig. S18). The characteristics of $Dkk1^+$ (–dox) GL261 tumors (Wnt inhibition) were compared with those of $Dkk1^-$ (+dox) tumors of mice injected with AAV-EGFP (control) or AAV-K190A (Wnt activation). We observed that $Dkk1^-$ cells behaved as wild-type GL261 cells, with ~95% of the AAV-K190A–treated $Dkk1^-$ tumors being smaller than 40 mm^3 at 20 to 24 dpi, and the AAV-EGFP cohort exhibiting more variable volumes (10 to 80 mm^3) (Fig. 6A). $Dkk1^+$ tumors grew even bigger, up to 160 mm^3. Endothelial Wnt activity markers (LEF1 and GLUT1) were the highest in the Wnt-stimulated $Dkk1^-$/K190A tumors and the lowest in Wnt inhibitory $Dkk1^+$ tumors, with $Dkk1^-$/EGFP tumors showing intermediate values (fig. S19, A and B). Hemorrhage (fig. S20), vascular density (fig. S19C), and fibrinogen leakage (Fig. 6B) followed the opposite trend, being gradually reduced by the stepwise increase in endothelial Wnt signaling.

Contrary to BBB restoration toward 350-kDa fibrinogen, small-molecule 557-Da sulfo-NHS-biotin leaked within all examined tumors, irrespective of their endothelial Wnt activation level. However, $Dkk1^+$ tumors exhibited slightly higher leakage values (Fig. 6C). To assess BBB repair to protein-sized tracers, we examined tumor and cortical vessels by electron microscopy after intravenous injection of 44-kDa horseradish peroxidase (HRP). In the healthy mouse cerebral cortices, HRP, revealed as an electron-dense 3,3′-diaminobenzidine reaction product, penetrated the intercellular spaces of adjacent ECs only over small distances. The signal sharply stopped at presumptive tight junctions (Fig. 6D, arrowheads), as reported previously (*34*). The electron density of the endothelial basement membranes was consequently much lower than the lumen. This spatially restricted distribution of HRP contrasted with almost all $Dkk1^+$ and most $Dkk1^-$/EGFP tumor vessels, in which the signal was observed along the entire length of the intercellular spaces. In these dysfunctional vessels, no difference was found between HRP levels within blood vessel lumens and their basement membranes. However, mice injected with AAV-K190A exhibited tumor vessels with a functional BBB phenotype. In line with the electron micrographs, claudin-5 immunostaining appeared denser in AAV-K190A tumor vessels (Fig. 6E). These findings are compatible with the hypothesis that AAV-K190A partially corrects the tight-junctional defects of glioblastoma vessels. On a cautionary note, however, we cannot formally exclude the possibility that the accumulation of HRP within the basement membranes and basolateral side of the inter-endothelial clefts results, at least in part, from HRP leaks associated with more distant hemorrhages.

The substantial intratumoral leak of HRP resulted in overall modest electron-dense contrast, making unambiguous scoring of transcytosis vesicles in glioblastoma vessels impractical. However, Mfsd2a, an endothelium-specific inhibitor of caveolae-mediated transcytosis (*34*), was increased by endothelial Wnt activation (Fig. 6F). Accordingly, caveolin-1 levels were lowered by AAV-K190A (fig. S21). The pericyte loss, typically associated with glioblastoma (*12*, *14*) and up-regulated transcytosis (*34*), could also be partially counteracted by AAV-K190A (Fig. 6G). Together, these findings show that in GL261 tumors, $Wnt7a^{K190A}$ restores endothelial Wnt signaling, reduces vascular density, and normalizes the BBB pleiotropically, thereby affecting both the transcellular and paracellular permeability routes and slowing tumor progression.

As proof of concept that the BBB-protective properties of the uncovered Gpr124/Reck agonists could have implications in CNS disorders of radically different etiology and BBB dysfunction kinetics, we turned to large-vessel and focal transient ischemic stroke models. After stroke, surgical or pharmacological recanalization therapies are crucial to promptly restore perfusion of the ischemic penumbra, a rim of cells whose survival will depend on the timing of recanalization. However, upon salutary blood flow restoration, reperfusion-associated tissue injury leads to BBB damage and contributes to worsening outcomes (*1*, *35*). To establish whether Gpr124/Reck-stimulated Wnt signaling at the BBB could mitigate the infarct size by limiting post-stroke injury, we subjected AAV-EGFP and AAV-K190A injected mice to transient middle cerebral artery occlusions (tMCAO). 2,3,5-Triphenyltetrazolium chloride (TTC) staining of whole-brain coronal sections revealed a significantly reduced infarct volume upon $Wnt7a^{K190A}$ expression (Fig. 6H). This reduction is consistent with previously reported effects of conditional endothelial β-catenin stabilization (*14*). A similar beneficial effect was observed in a transient focal endothelin-1 (ET-1) stroke model but not in a permanent photothrombotic (PT) stroke model (Fig. 6I); hence, we tentatively assign the protective effects of $Wnt7a^{K190A}$ to the post-stroke reperfusion process.

Discussion

Our study has revealed that Wnt7a ligands can be engineered into highly specific Gpr124/Reck agonists, thereby disclosing a novel class of BBB therapeutics. This level of specificity was deemed unreachable for Wnt-derived proteins by virtue of their promiscuous mode

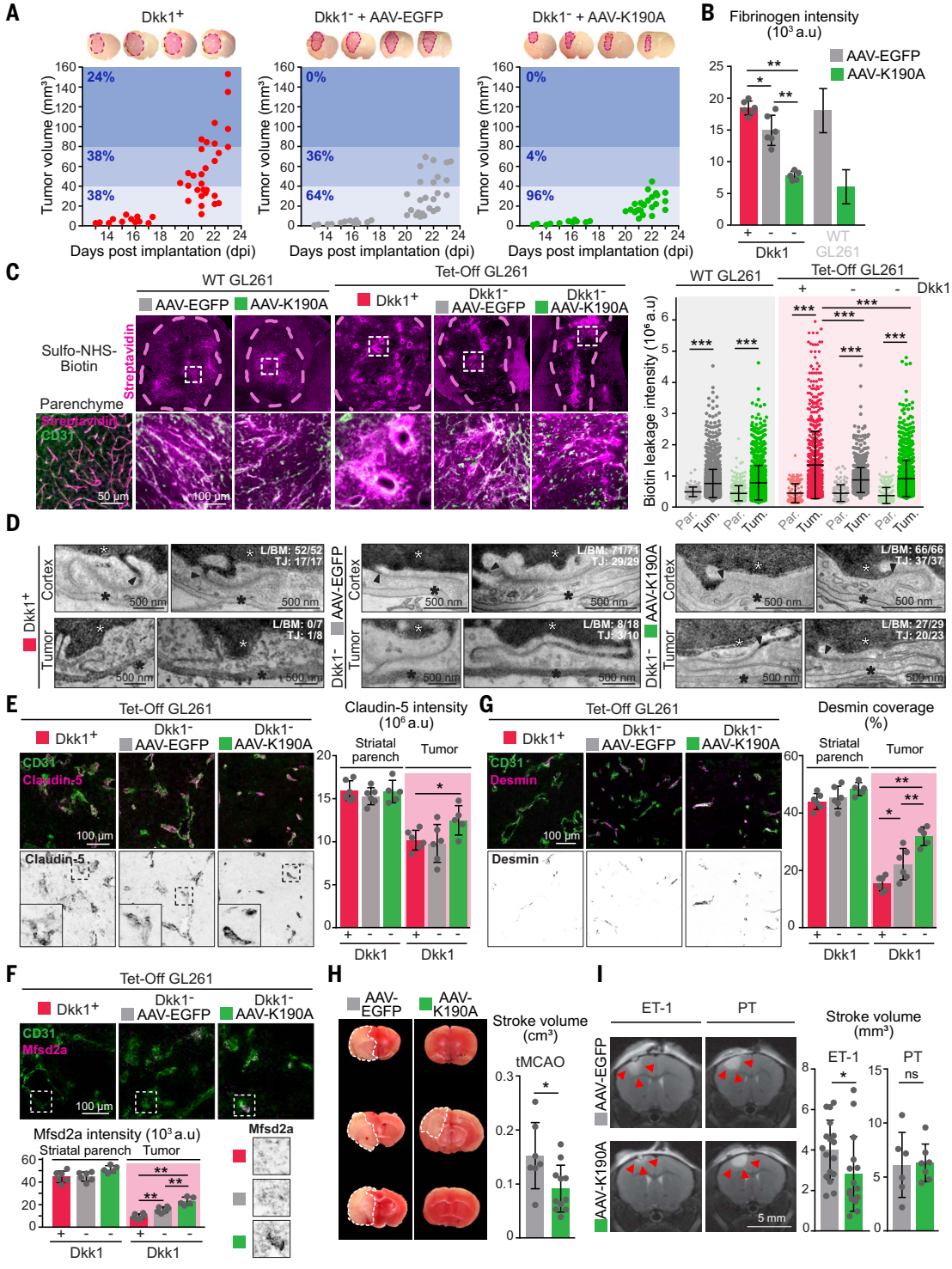

Fig. 6. Gpr124/Reck agonists as BBB repair agents in glioblastoma and stroke models. (**A**) MRI monitoring of tumor volumes after implantation of 1×10^5 Tet-Off Dkk1 GL261 cells, in the absence of doxycycline (Dkk1$^+$, –dox) or the presence of doxycycline (Dkk1$^-$, +dox). Doxycycline-exposed mice were injected intravenously with AAV-EGFP or AAV-K190A as indicated. (**B**) Quantification of fibrinogen leakage into the tumor. Data for WT GL261 are the same as in Fig. 5G. (**C**) Leakage of transcardially perfused sulfo-NHS-biotin within the tumor (Tum.) and the healthy parenchyma (Par.). The dashed lines highlight the tumor margin. (**D**) Electron micrographs of tumor and cortical sections of HRP-injected mice. White and black asterisks indicate tracer within the vessel lumen and vascular basement membrane, respectively. Proportions of vessels with high lumen–basement membrane HRP ratios (L/BM) and functional tight junctions (TJ) are indicated. Arrowheads label the tight junctions kissing points. (**E** to **G**) Coimmunostaining of CD31 together with claudin-5 (E), Mfsd2a (F), or desmin (G). (**H** and **I**) Infarct volumes of AAV-injected mice subjected to tMCAO [(H), TTC-stained sections, 24 hours after stroke], transient focal endothelin-1 stroke [(I), ET-1, MRI scans, 48 hours after stroke] or permanent bengal rose photothrombotic stroke [(I), PT, MRI scans, 48 hours after stroke]. Data are means ± SD. *P < 0.05, **P < 0.01, ***P < 0.001.

of interaction with the widely expressed Fz receptors.

In contrast to Wnt7a, the uncovered Gpr124/Reck agonists were well tolerated in vivo despite the broad expression strategies adopted in this study. In *Xenopus* and zebrafish, their ubiquitous expression during early development did not cause morphological alterations. In mice, CNS-wide expression of Gpr124/Reck agonists did not trigger ectopic Wnt activation or detectable adverse phenotypes. In addition to their strict signaling specificity, we suspect that homeostatic feedback loops maintain Wnt signaling within carefully controlled physiological activity windows. Accordingly, we detected increased endothelial Wnt signaling only in dysfunctional BBB vessels, leaving healthy parenchymal vessels unaffected.

Alternative strategies are being pursued to restore BBB function in disease, including those relying on protein C–mediated activation of endothelial PAR-1 signaling (*36*) or PDGF-C inhibition within the neurovascular unit (*37*). As a contrasting strategy to these

approaches, we here repurposed a key developmental BBB-inductive signal, acting at the top of the differentiation cascade that primes ECs for BBB development. As also reflected in this study, Wnt/β-catenin has been implicated in many aspects of BBB physiology. These include expression of tight junction proteins and solute transporters, suppression of vesicular transport, reduction of plasmalemma vesicle-associated protein (PLVAP) expression, and pericyte recruitment via control of PDGF-B secretion levels (*7*–*12*). Such a pleiotropic impact on BBB function seems well positioned to initiate a productive repair process. Despite this potential, Gpr124/Reck agonists are lipophilic, complicating their recombinant production at scale.

The therapeutic scope of Gpr124/Reck agonists is possibly large but remains to be functionally explored. Indeed, although the glioblastoma endothelium displays an aberrant Wnt expression profile (*14*), the post-stroke endothelium does not (*35*, *38*). Instead, multiple etiologically distinct disorders converge to a common diseased BBB transcriptomic signature reminiscent of peripheral endothelia (*38*). This observation suggests that reshaping the neurovascular niche by reinforcing the priming Gpr124/Reck-activating signal will likely have a broader impact than what can rationally be inferred from transcript profiling or biomarker analysis.

Our work defines a modality to treat CNS disorders by repairing the BBB. BBB-focused intervention strategies have potential as disease-modifying or secondary prevention agents in various pathologies beyond those explored in this study, including multiple sclerosis, epilepsy, and neurodegenerative disorders such as Alzheimer's disease.

Methods summary

Throughout this study, Wnt ligands and their variants were C-terminally tagged (V5 or P2A fusions). In cellular assays, ligands and co-receptor components were transiently expressed from CMV promoters. Firefly luciferase activities (derived from a genomic transgene in STF cells or ectopically expressed from the transfected M50 Super 8x TOPFlash plasmid) were normalized to Renilla luciferase activities (pTK-Renilla vector transfection). Immunodetection of extracellular and intracellular Wnt7a was performed using distinct antibodies (anti-Wnt7a and anti-V5) before and after cell permeabilization. Zebrafish and *Xenopus* were injected respectively at the 1-cell and 4-cell stage with in vitro transcribed V5-tagged Wnt7a mRNA or variants thereof. Transgenic endothelial expression in zebrafish was achieved using the Tol2 transposase system. In mice, Wnt7a or variants thereof were expressed using PHP.eB AAV particles and CAG promoters. AAVs were delivered retro-orbitally or by tail vein injections. The Dkk1 Tet-Off GL261 cells were cultured in media supplemented or not with doxycycline (1 μg/ml) for 5 days before implantation. To implant tumor cells, anesthetized mice were placed into a stereotactic device, and 2 μl of PBS containing 105 living GL261 cells were injected at 0.25 μl/min into the striatum. For Tet-Off–dependent experiments, mice were fed with control diet or diet containing doxycycline hyclate (1 g/kg) starting 2 weeks before the implantation. To evaluate BBB permeability, EZ-Link-Sulfo-NHS-Biotin was perfused intracardially and HRP was injected retro-orbitally. Electron microscopy was performed after DAB revelation of brain sections from HRP-injected mice. Transient MCAO was performed by a 1-hour occlusion of the right MCA using standardized monofilament 24 hours prior to tissue harvesting for TTC staining. PT stroke was induced by a 530-nm laser exposure of Rose Bengal–injected mice for 10 min. ET-1–induced stroke was achieved by a stereotaxic injection of 1 μl of 800 pmol ET-1 in the motor cortex. PT and ET-1 infarct volumes were monitored using magnetic resonance imaging 48 hours after stroke. Categorical phenotypic assessments were performed by researchers blind to the experimental conditions.

REFERENCES AND NOTES

1. B. Obermeier, R. Daneman, R. M. Ransohoff, Development, maintenance and disruption of the blood-brain barrier. *Nat. Med.* **19**, 1584–1596 (2013). doi: 10.1038/nm.3407; pmid: 24309662
2. B. W. Chow, C. Gu, The molecular constituents of the blood-brain barrier. *Trends Neurosci.* **38**, 598–608 (2015). doi: 10.1016/j.tins.2015.08.003; pmid: 26442694
3. Z. Zhao, A. R. Nelson, C. Betsholtz, B. V. Zlokovic, Establishment and Dysfunction of the Blood-Brain Barrier. *Cell* **163**, 1064–1078 (2015). doi: 10.1016/j.cell.2015.10.067; pmid: 26590417
4. M. D. Sweeney, Z. Zhao, A. Montagne, A. R. Nelson, B. V. Zlokovic, Blood-Brain Barrier: From Physiology to Disease and Back. *Physiol. Rev.* **99**, 21–78 (2019). doi: 10.1152/physrev.00050.2017; pmid: 30280653
5. C. P. Profaci, R. N. Munji, R. S. Pulido, R. Daneman, The blood-brain barrier in health and disease: Important unanswered questions. *J. Exp. Med.* **217**, e20190062 (2020). doi: 10.1084/jem.20190062; pmid: 32211826
6. U. Lendahl, P. Nilsson, C. Betsholtz, Emerging links between cerebrovascular and neurodegenerative diseases-a special role for pericytes. *EMBO Rep.* **20**, e48070 (2019). doi: 10.15252/embr.201948070; pmid: 31617312
7. S. Liebner *et al.*, Wnt/β-catenin signaling controls development of the blood-brain barrier. *J. Cell Biol.* **183**, 409–417 (2008). doi: 10.1083/jcb.200806024; pmid: 18955553
8. J. M. Stenman *et al.*, Canonical Wnt signaling regulates organ-specific assembly and differentiation of CNS vasculature. *Science* **322**, 1247–1250 (2008). doi: 10.1126/science.1164594; pmid: 19023080
9. R. Daneman *et al.*, Wnt/β-catenin signaling is required for CNS, but not non-CNS, angiogenesis. *Proc. Natl. Acad. Sci. U.S.A.* **106**, 641–646 (2009). doi: 10.1073/pnas.0805165106; pmid: 19129494
10. Y. Wang *et al.*, Norrin/Frizzled4 signaling in retinal vascular development and blood brain barrier plasticity. *Cell* **151**, 1332–1344 (2012). doi: 10.1016/j.cell.2012.10.042; pmid: 23217714
11. Y. Zhou *et al.*, Canonical WNT signaling components in vascular development and barrier formation. *J. Clin. Invest.* **124**, 3825–3846 (2014). doi: 10.1172/JCI76431; pmid: 25083995
12. M. Reis *et al.*, Endothelial Wnt/β-catenin signaling inhibits glioma angiogenesis and normalizes tumor blood vessels by inducing PDGF-B expression. *J. Exp. Med.* **209**, 1611–1627 (2012). doi: 10.1084/jem.20111580; pmid: 22908324
13. J. E. Lengfeld *et al.*, Endothelial Wnt/β-catenin signaling reduces immune cell infiltration in multiple sclerosis. *Proc. Natl. Acad. Sci. U.S.A.* **114**, E1168–E1177 (2017). doi: 10.1073/pnas.1609905114; pmid: 28137846
14. J. Chang *et al.*, Gpr124 is essential for blood-brain barrier integrity in central nervous system disease. *Nat. Med.* **23**, 450–460 (2017). doi: 10.1038/nm.4309; pmid: 28288111
15. C. Y. Janda, D. Waghray, A. M. Levin, C. Thomas, K. C. Garcia, Structural basis of Wnt recognition by Frizzled. *Science* **337**, 59–64 (2012). doi: 10.1126/science.1222879; pmid: 22653731
16. R. Nusse, H. Clevers, Wnt/β-Catenin Signaling, Disease, and Emerging Therapeutic Modalities. *Cell* **169**, 985–999 (2017). doi: 10.1016/j.cell.2017.05.016; pmid: 28575679
17. B. Vanhollebeke *et al.*, Tip cell-specific requirement for an atypical Gpr124- and Reck-dependent Wnt/β-catenin pathway during brain angiogenesis. *eLife* **4**, e06489 (2015). doi: 10.7554/eLife.06489; pmid: 26051822
18. C. Cho, P. M. Smallwood, J. Nathans, Reck and Gpr124 Are Essential Receptor Cofactors for Wnt7a/Wnt7b-Specific Signaling in Mammalian CNS Angiogenesis and Blood-Brain Barrier Regulation. *Neuron* **95**, 1056–1073.e5 (2017). doi: 10.1016/j.neuron.2017.07.031; pmid: 28803732
19. M. Eubelen *et al.*, A molecular mechanism for Wnt ligand-specific signaling. *Science* **361**, eaat1178 (2018). doi: 10.1126/science.aat1178; pmid: 30026314
20. M. Vallon *et al.*, A RECK-WNT7 Receptor-Ligand Interaction Enables Isoform-Specific Regulation of Wnt Bioavailability. *Cell Rep.* **25**, 339–349.e9 (2018). doi: 10.1016/j.celrep.2018.09.045; pmid: 30304675
21. C. Cho, Y. Wang, P. M. Smallwood, J. Williams, J. Nathans, Molecular determinants in Frizzled, Reck, and Wnt7a for ligand-specific signaling in neurovascular development. *eLife* **8**, e47300 (2019). doi: 10.7554/eLife.47300; pmid: 31225798
22. X. Zhang *et al.*, Tiki1 is required for head formation via Wnt cleavage-oxidation and inactivation. *Cell* **149**, 1565–1577 (2012). doi: 10.1016/j.cell.2012.04.039; pmid: 22726442
23. X. Zhang *et al.*, Notum is required for neural and head induction via Wnt deacylation, oxidation, and inactivation. *Dev. Cell* **32**, 719–730 (2015). doi: 10.1016/j.devcel.2015.014; pmid: 25771893
24. H. Li *et al.*, RECK in Neural Precursor Cells Plays a Critical Role in Mouse Forebrain Angiogenesis. *iScience* **19**, 559–571 (2019). doi: 10.1016/j.isci.2019.08.009; pmid: 31445376
25. S. Eisa-Beygi, G. Hatch, S. Noble, M. Ekker, T. W. Moon, The 3-hydroxy-3-methylglutaryl-CoA reductase (HMGCR) pathway regulates developmental cerebral-vascular stability via prenylation-dependent signalling pathway. *Dev. Biol.* **373**, 258–266 (2013). doi: 10.1016/j.ydbio.2012.11.024; pmid: 23206891
26. K. Y. Chan *et al.*, Engineered AAVs for efficient noninvasive gene delivery to the central and peripheral nervous systems. *Nat. Neurosci.* **20**, 1172–1179 (2017). doi: 10.1038/nn.4593; pmid: 28671695
27. N. A. Jessen, A. S. F. Munk, I. Lundgaard, M. Nedergaard, The Glymphatic System: A Beginner's Guide. *Neurochem. Res.* **40**, 2583–2599 (2015). doi: 10.1007/s11064-015-1581-6; pmid: 25947369
28. S. Maretto *et al.*, Mapping Wnt/β-catenin signaling during mouse development and in colorectal tumors. *Proc. Natl. Acad. Sci. U.S.A.* **100**, 3299–3304 (2003). doi: 10.1073/pnas.0434590100; pmid: 12626757
29. C. Liu, Y. Wang, P. M. Smallwood, J. Nathans, An essential role for Frizzled5 in neuronal survival in the parafascicular nucleus of the thalamus. *J. Neurosci.* **28**, 5641–5653 (2008). doi: 10.1523/JNEUROSCI.1056-08.2008; pmid: 18509025
30. M. Sahores, A. Gibb, P. C. Salinas, Frizzled-5, a receptor for the synaptic organizer Wnt7a, regulates activity-mediated synaptogenesis. *Development* **137**, 2215–2225 (2010). doi: 10.1242/dev.046722; pmid: 20530549
31. M. Corada *et al.*, Fine-Tuning of Sox17 and Canonical Wnt Coordinates the Permeability Properties of the Blood-Brain Barrier. *Circ. Res.* **124**, 511–525 (2019). doi: 10.1161/CIRCRESAHA.118.313316; pmid: 30591003
32. T. N. Phoenix *et al.*, Medulloblastoma Genotype Dictates Blood Brain Barrier Phenotype. *Cancer Cell* **29**, 508–522 (2016). doi: 10.1016/j.ccell.2016.03.002; pmid: 27050100
33. A. Griveau *et al.*, A Glial Signature and Wnt7 Signaling Regulate Glioma-Vascular Interactions and Tumor Microenvironment.

Cancer Cell **33**, 874–889.e7 (2018). doi: 10.1016/j.ccell.2018.03.020; pmid: 29681511
34. A. Ben-Zvi *et al*., Mfsd2a is critical for the formation and function of the blood-brain barrier. *Nature* **509**, 507–511 (2014). doi: 10.1038/nature13324; pmid: 24828040
35. R.-I. Kestner *et al*., Gene Expression Dynamics at the Neurovascular Unit During Early Regeneration After Cerebral Ischemia/Reperfusion Injury in Mice. *Front. Neurosci.* **14**, 280 (2020). doi: 10.3389/fnins.2020.00280; pmid: 32300291
36. J. H. Griffin, J. A. Fernández, P. D. Lyden, B. V. Zlokovic, Activated protein C promotes neuroprotection: Mechanisms and translation to the clinic. *Thromb. Res.* **141** (Suppl 2), S62–S64 (2016). doi: 10.1016/S0049-3848(16)30368-1; pmid: 27207428
37. S. A. Lewandowski, L. Fredriksson, D. A. Lawrence, U. Eriksson, Pharmacological targeting of the PDGF-CC signaling pathway for blood-brain barrier restoration in neurological disorders. *Pharmacol. Ther.* **167**, 108–119 (2016). doi: 10.1016/j.pharmthera.2016.07.016; pmid: 27524729
38. R. N. Munji *et al*., Profiling the mouse brain endothelial transcriptome in health and disease models reveals a core blood-brain barrier dysfunction module. *Nat. Neurosci.* **22**, 1892–1902 (2019). doi: 10.1038/s41593-019-0497-x; pmid: 31611708

ACKNOWLEDGMENTS

We thank C. Hénin, L. Conrard, E. Zindy, G. Oldenhove, M. Moser, F. Andris, M. I. Garcia, K. Somme, M. S. Jeffers, G. O. Cron, O. A. Stone, P. Gut, and D. Y. R. Stainier for their help, and D. L. Silver and V. Gradinaru for the anti-Mfsd2a antibodies and the PHP.eB construct (Addgene plasmid #103005), respectively. The summary page figure and the illustration of Fig. 4A were created with BioRender.com. **Funding:** M.E., and N.B. are FRIA fellows, A.D.G. is FNRS-L'Oreal fellow, and S.V. and P.C. are postdoctoral researchers of the FRS-FNRS. Work in the B.V. laboratory is supported by the FNRS (MIS F.4543.15), the Concerted Research Action, the Fondation ULB, the H2020 ITN "BtRAIN," the Queen Elisabeth Medical Foundation, the FRFS-WELBIO (CR-2017S-05R), and the ERC (CtrI-BBB 865176). Also supported by DFG grant LI 911/5-1, LI 911/7-1, the Excellence Cluster Cardio-Pulmonary Institute, the H2020 ITN "BtRAIN," the DZHK, and the LOEWE CePTER Epilepsy Research Center of the state Hesse (S.L. and K.D.) and by Heart and Stroke Foundation of Canada grant G-17-0018290, Canadian Institute of Health Research grant 388805, and New Frontiers Research Funds-Exploration grant NFRFE-2019-00641 (B.L.). A.d.K.d'E. is research director of FRS-FNRS, supported by FRS-FNRS and the Fondation Clerdent. The Center for Microscopy and Molecular Imaging is supported by the European Regional Development Fund and the Walloon Region. **Author contributions:** All authors performed research and/or analyzed data. All authors discussed results and edited the manuscript. M.M. and B.V. wrote the manuscript. B.V. supervised the study. **Competing interests:** The ULB (B.V.) has filed for patent protection for Gpr124/Reck-specific agonism. B.V. is a founder, shareholder, and consultant of NeuVasQ Biotechnologies. **Data and materials availability:** All data are available in the main text or the supplementary materials.

SUPPLEMENTARY MATERIALS

23 September 2021; accepted 14 December 2021
10.1126/science.abm4459

Science

Engineered Wnt ligands enable blood-brain barrier repair in neurological disorders

Maud MartinSimon VermeirenNaguissa BostailleMarie EubelenDaniel SpitzerMarjorie VermeerschCaterina P. ProfaciElisa PozueloXavier ToussayJoanna Raman-NairPatricia TebabiMichelle AmericaAurélie De GrooteLeslie E. SandersonPauline CabochetteRaoul F. V. GermanoDavid TorresSébastien BoutryAlban de Kerchove d'ExaerdeEric J. BellefroidTimothy N. PhoenixKavi DevrajBaptiste LacosteRichard DanemanStefan LiebnerBenoit Vanhollebeke

Science, 375 (6582), eabm4459. • DOI: 10.1126/science.abm4459

Endothelial-targeted BBB therapeutics

The brain is protected not only by the skull, but also by the blood–brain barrier (BBB), which restricts transmission of substances from the blood into the central nervous system (CNS) extracellular fluid. If the BBB is breached, then neurological disorders result. Therefore, it is desirable to develop intervention strategies that correct BBB deficits by restoring its function. Wnt signaling proteins have been shown to regulate the BBB, and Martin *et al*. developed a large, single-residue mutational screen covering more than half of the exposed surface of Wnt7a (see the Perspective by McMahon and Ichida). They identified a class of variants that exhibit strict specificity for the BBB's Gpr124/Reck Wnt signaling module. Gpr124/Reck agonists display "on-target" neurovascular protective properties in stroke and glioblastoma models in mice without "off-target" Wnt activation in other tissues, thereby defining a strategy to alleviate CNS disorders by repairing the BBB. —BAP